*Int. J. Electrochem. Sci.*, 10 **(2015)** 9632 - 9640

International Journal of
ELECTROCHEMICAL
SCIENCE
www.electrochemsci.org

# One-pot Preparation of Reduced Graphene Oxide/Silver Nanocomposite and Its Application in the Electrochemical Determination of 4-Nitrophenol

*Guoqiang Yang*

Clinical laboratory, People Hospital of Zhengzhou, P. R. China
E-mail: guoqiangyang_2013@126.com

*Received:* 24 August 2015 / *Accepted:* 12 September 2015 / *Published:* 30 September 2015

A novel electrochemical sensor was fabricated using reduced graphene oxide (RGO) and Ag nanoparticle composite (RGO-Ag). The nanocomposite was synthesized via a facial simple one-pot hydrothermal method. The synthesized nanocomposite was characterized by a series techniques. The synthesized RGO-Ag nanocomposite has been used as an electrode modifier. The fabricated electrode was used for sensitive and selective determination of 4-NP. The proposed sensor exhibited a linear dependence on 4-NP concentration range from 1 to 500 μM with a low detection limit of 0.114 μM. In addition, our proposed 4-NP sensor also exhibited an outstanding stability, reproducibility and anti-interference property.

**Keywords:** Reduced graphene oxide; Ag NPs; 4-nitrophenol; Sensor; Electrochemistry

## 1. INTRODUCTION

4-Nitrophenol (4-NP), an aromatic phenolic compound, is one of the toxic substances commonly used as pesticide and insecticide [1-3]. Due to its highly toxicity to both environment and human health, 4-nitrophenol has been included in the Environmental Protection Agency List of Priority Pollutants. Therefore, the monitoring and selective determination of 4-NP becomes more significant to both environmental and human safety aspects. Up to now, many analytical method has been developed for determining 4-NP, such as spectrophotometry [4], fluorescence [5], high performance liquid chromatography [6-10], capillary zone electrophoresis [11] and electrochemical techniques [12-17]. Among these techniques, electrochemical method was found to have advantages of fast response, cost effective instrument, simple operation, time saving, high sensitivity and selectivity, real-time detection for real samples [2, 18-21]. However, the electrochemical reduction of 4-NP at a bare electrode is generally difficult and needs a high overpotential. Therefore, electrode surface

modification is commonly adopted for enhancing analytic performance. For example, Yin et al.[22] reported a 4-NP sensor based on a glassy carbon electrode (GCE) modified with a hydroxyapatite nanopowder. The modified electrode showed a detection linear range of 4-NP from 1.0 μM to 300 μM with a detection limit of 0.6 μM. Sing et al.[23] reported a 4-NP sensor based on $CeO_2$–ZnO nanoellipsoids modified GCE. The proposed sensor showed a reproducible sensitivity of ~0.120 μA/nM $cm^2$ and detection limit of 1.163 μM.

Recently, graphene, a two-dimensional $sp^2$-hybridized carbon material, has attracted attention of various research groups as it exhibited excellent charge transport mobility, large specific surface area, high electrocatalytic activity and low cost [24-27]. Due to these properties, graphene has been used for a new carbon based electrocatalysts for sensing applications. Several reports have been conducted for using graphene to fabrication of 4-NP electrochemical sensors [28, 29]. For example, Li and coworkers demonstrated using graphene oxide (GO) film coated GCE as a sensitive electrochemical sensor for 4-NP detection [30]. Under the optimal conditions, the fabricated sensor has a linear detection range from 0.1 to 120 μM with a detection limit of 0.02 μM. On the other hand, nanostructured silver (Ag) has also been explored to modify electrodes for electrochemical sensors [31, 32]. Moreover, the electrocatalytic activity of Ag could be further enhanced when supported on graphene or its derivatives due to the synergic effect provide by two substances [33, 34]. For example, Wu and co-workers reported fabrication of silver-graphene oxide nanocomposite for electrochemical determination of α-1-fetoprotein [35]. Zhao and coworkers reported construction of 3D electrochemically reduced graphene oxide–silver nanocomposite film for nonenzymatic hydrogen peroxide determination [36].

Herein, we prepared a reduced graphene oxide/Ag nanocomposite (RGO-Ag) via a simple one-pot hydrothermal method using graphene oxide and $AgNO_3$ as starting materials. The synthesized nanocomposite was characterized by UV-vis spectroscopy, SEM, EDX, XRD and Raman spectroscopy. The Ag NPs are uniformly distributed on the surface of the RGO sheets. We also demonstrate here the excellent electrocatalytic activity of the RGO-Ag nanocomposite modified electrode in detection of 4-NP.

## 2. EXPERIMENTS

### *2.1 Materials*

Synthetic graphite (average particle diameter <20 μm), silver nitrate ($AgNO_3$), ammonium hydroxide (28-30% $NH_3$ basis), urea and 4-NP were purchased from Sigma-Aldrich.

### *2.2 Preparation of RGO-Ag nanocomposite*

Graphene oxide was synthesized by modified Hummer's approach [37-40]. GO (10 mg) was added into 120 mL water by 1 h ultrasound under ambient condition, then 5 mL of $AgNO_3$ (20 mM) was added to the dispersion for further 1 h ultrasound. Then, 0.1 g urea was added into above dispersion under stirring. The result suspension was adjusted to pH 9 by ammonia and then transferred to a 50 mL Teflon-lined stainless steel autoclave. The autoclave was heated to 140°C and maintained

for 6 h in an oven and cooled down to the room temperature. The final product was obtained after drying in an oven at 70°C for 12 h

### *2.3 Characterization*

Surface morphology of prepared samples were observed by a SEM (S-4700, HITACHI). The optical properties of sample was characterized by a UV-vis spectrophotometer. X-ray diffraction patterns were collected from 5° to 80° in 2θ by a XRD with Cu Kα radiation (D8-Advanced, Bruker). Raman analysis was carried out at room temperature using a Raman spectroscope (Renishaw InVia, UK) with a 514 nm laser light.

### *2.4 Electrochemical determiantion*

For electrochemical test, a GCE was polished first using alumina. The surface modification process contains follow procedure, 5 μL of modifier dispersion(0.5 mg/mL) was placed on the electrode surface and dried naturally. A CH Instruments 660A electrochemical Workstation (CH Instruments, USA) was used for electrochemical test under three electrodes mode. The auxiliary electrode is a platinum electrode. The reference electrode is a 3M Ag/AgCl electrode.

## 3. RESULTS AND DISCUSSION

### *3.1 Characterization of RGO-Ag nanocomposite*

Figure 1A depicts the UV-vis spectra of GO and RGO-Ag dispersion. The GO spectrum exhibits a absorption peak at 228 nm corresponding to the π→π* transition of aromatic C═C bonds [41]. After hydrothermal reaction, this peak red-shifts to 260 nm in the spectrum of RGO-Ag, indicating the GO has been reduced to RGO [42, 43]. Moreover, the spectrum of RGO-Ag also shows a clear broad absorption peak centred at 600 nm, which is due to the surface plasmon resonance provide by Ag NPs, indicating the successful construction of Ag NPs.

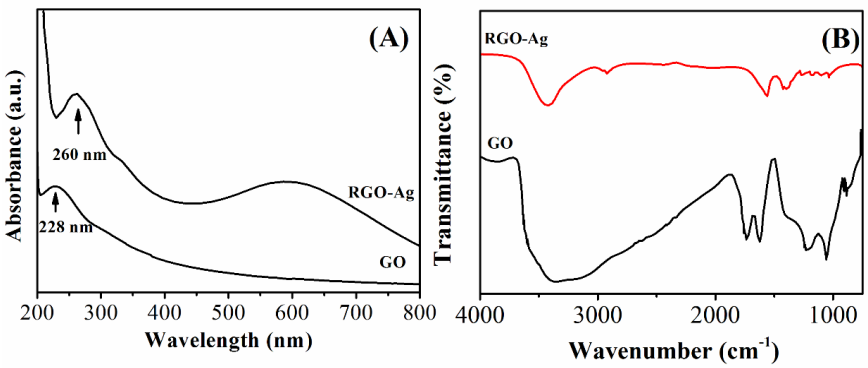


**Figure 1.** (A) UV-vis spectra of GO and RGO-Ag nanocoposite. (B) FTIR spectra of GO and RGO-Ag nanocomposite.

The reduction of GO was further characterized by FTIR. Figure 1B displays the FTIR spectra of pure GO and prepared RGO-Ag nanocomposite. As excepted, GO spectrum displays peaks at 3392, 1731, 1620, 1224, 1052 and 855 $cm^{-1}$, corresponding to the ─OH stretching, C–O stretching vibrations of the COOH functional groups, the graphitic domains vibration, C─OH stretching vibrations, C–O stretching and C–O–C vibration, respectively [44]. After hydrothermal treatment, these finger prints of GO decreased or even vanished in the term of RGO-Ag nanocomposite, indicating the occurance of the reduction process.

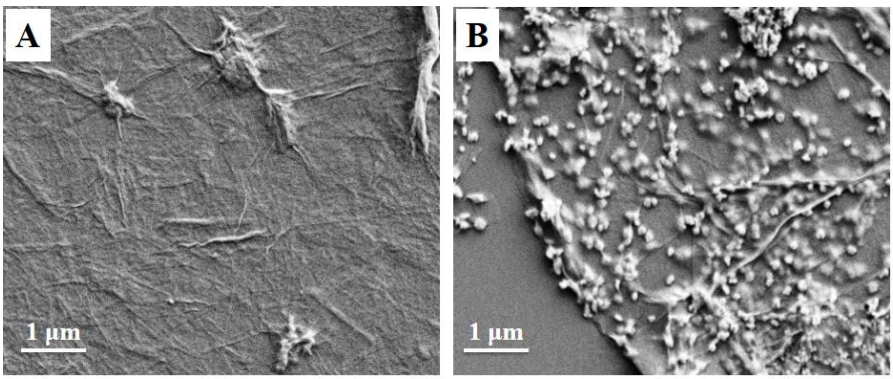


**Figure 2.** SEM image of (A) GO and (B) RGO-Ag nanocomposite.

The morphology of as-prepared samples were subsequently observed by SEM. Figure 2 displays the typical SEM images of GO and RGO-Ag nanocomposites. In comparison with the bare GO sheets (Figure 2A), the RGO-Ag nanocomposite (Figure 2B) exhibits a uniform decoration of Ag NPs on both sides of the RGO sheets. The average size of Ag particles is about 90 nm (based on more than 200 Ag nanoparticles). It is noteworthy that the decoration of Ag NPs on the RGO sheet surface can prevent the re-stacking phenomenon of RGO sheets [45]. The result RGO-Ag showed no precipitate over two months.

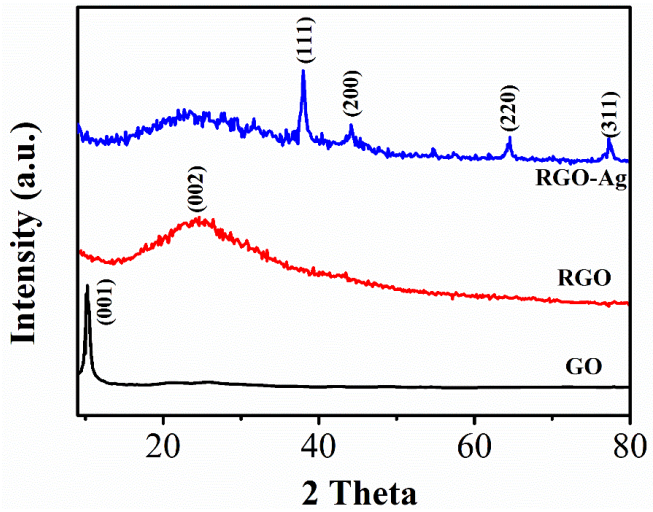


**Figure 3.** XRD patterns of GO, RGO and RGO-Ag nanocomposite.

The crystalline structure of GO, RGO and RGO-Ag nanocomposite was analyzed by XRD and depicted in Figure 3. It can be seen that the pristine GO displays a typical characteristic (001) peak at 11.1° with a *d*-spacing value of 0.79 nm [46]. The disappearance of the (0 0 1) peak indicates the occurrence of reduction of GO and an appearance of a broad peak at 23.4°, suggesting the presence of stacked graphene layers of RGO [47]. Moreover, the diffraction peaks at 36.40°, 42.57°, 62.83°, and 75.81° are assigned to the (200), (220), (311) and (222) silver face-centered-cube (fcc) crystal diffractions (JCPDS file no. 04-0783), respectively.

### *3.2 Electrochemical determination of 4-NP*

In order to characterization of electrochemical properties of as-prepared electrode, cyclic voltammograms (CVs) of bare GCE, RGO and RGO-Ag nanocomposite modified GCEs were taken in PBS. Figure 4A shows no redox peak is observed for the RGO-GCE and bare GCE. In contrast, a pair of well-defined redox peaks are observed in the RGO-Ag modified GCE, corresponding to $Ag/Ag^+$ redox couple. The peak at 0.61 V can be ascribed to the oxidation of $Ag(0) \rightarrow Ag^+$, whereas the reduction of $Ag^+ \rightarrow Ag(0)$ exhibits a peak at 0.08 V [48].

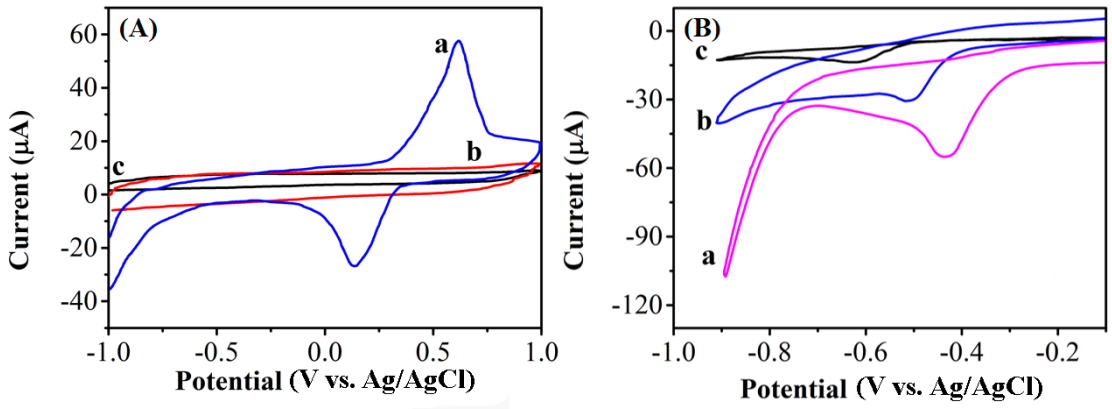


**Figure 4.** (A) CVs of (a) RGO-Ag nanocomposite, (b) RGO and (c) bare GCEs in PBS. (B): CVs of 0.2 mM 4-NP in PBS at the (a) a) RGO-Ag nanocomposite, (b) RGO and (c) bare GCEs.

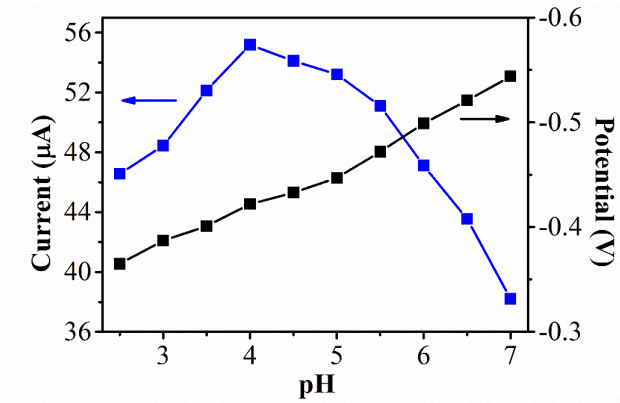


**Figure 5.** Effect of the pH of PBS on the current and potential response of 0.2 mM 4-NP at RGO-Ag nanocomposite modified GCE.

The electrochemical behavior of proposed sensor towards reduction of 4-NP was investigated using CV in pH 4.0 PBS solution. Figure 4B shows the CVs of bare, RGO and RGO-Ag modified GCEs towards electro-reduction of 4-NPs. Well-defined reduction peaks are shown at each electrode, suggesting the 4-NP undergoes an irreversible reaction.

The reduction peak of 4-NP using bare GCE is located at ─0.628 V with a peak current of 14.01 μA. The reduction peak of 4-NP using RGO modified GCE is located at ─0.507 V with a peak current of 29.82 μA, indicating the RGO sheets could promote electron transfer between the 4-NP molecules and electrode surface. However, at the RGO-Ag modified GCE, the peak current of 4-NP increases to 55.19 μA, and the overpotential is 75 mV lower compared with that of the RGO modified GCE. Therefore, the RGO-Ag nanocomposite can be used for catalyze the electrochemical reduction of 4-NP by their synergistic effect.[49]

Figure 5 shows the effect of pH on the reduction peak current. It can be clearly seen that the reduction current increases with the increasing of the pH from 2.5 to 4. At higher pH conditions, the reduction current start decreased. So, pH 4.0 was used as the optimum pH condition for this work. Figure 5 also shows the relationship between the reduction peak potential and pH. As can be observed, with increasing pH from 2.5 to 7.0, the reduction potential shifts negatively and linearly. The linear regression equation can be express as: $E_{pa}$ = -0.038 pH + 0.264 ($R^2$ = 0.994). Then, the ratio of the proton number against the transfer electron number can be according to the following formula:

$$dE_{pa}/dpH=(-2.303mRT)/nF$$

Where m is the proton number, n is the transfer electron number, R, T and F are constant numbers. Therefore, the proton number is calculated to be 0.87 and approximately equaled to 1, suggesting that the number of electrons and protons is equal. Therefore, a possible reduction process can be express as:

$$HOC_6H_4NO_2 + 4H^+ + 4e^- \longrightarrow HOC_6H_4NHOH + H_2O$$

Figure 6 displays the amperometric response upon additions of 4-NP at RGO-Ag nanocomposite modified GEC.

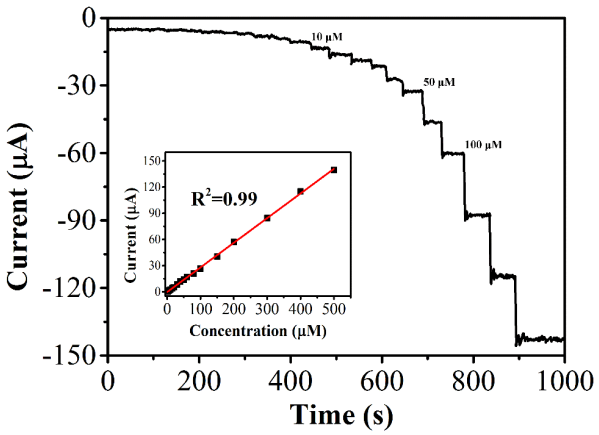


**Figure 6.** I-T curve of 4-NP in PBS at the RGO-Ag nanocomposite modified GCE using a working potential of ─0.4 V. Inset: the corresponding calibration curve.

The electrode potential was set as −0.4 V. Results showed that the RGO-Ag nanocomposite modified GCE could reach steady state current within in 4 s, indicating the prepared sensor has a rapid response towards 4-NP. The current values are proportional to the concentration in the ranges of 1 and 500 μM (Inset of Figure 6). The linear regression equation can be represented as: $I$ (μA) = 0.28258 C(μM) + -0.2756 ($R^2$ = 0.9981). The detection limit was calculated to be 0.114 μM (S/N = 3).

The reproducibility of the proposed 4-NP sensor were tested by looking the detection peak current of 0.2 mM 4-NP for ten modified electrodes. The relative standard deviation (RSD) was 3.25%, suggesting our demonstrated electrochemical sensor owing a good reproducibility. The stability of the proposed sensor was evaluated measuring the current response with 0.2 mM 4-NP every day over two weeks. The current response only decreased about 13% over two weeks, indicating the proposed sensor also has an acceptable storage stability. Table 1 summarize the each day detection results. In order to characterize our proposed sensor for real application, we collected drinking water, lake water, river water and underground water as samples for 4-NP detection (Table 2).

**Table 1.** 4-NP detection stability test using RGO-Ag nanocomposite modified GCE.

| Day | Current response | Day | Current response |
|---|---|---|---|
| 1 | 100% | 8 | 94.0% |
| 2 | 96.6% | 9 | 93.2% |
| 3 | 96.7% | 10 | 91.2% |
| 4 | 95.7% | 11 | 88.9% |
| 5 | 95.3% | 12 | 89.7% |
| 6 | 94.9% | 13 | 87.2% |
| 7 | 94.5% | 14 | 86.8% |

**Table 2.** Detection of 4-NP in different water samples using RGO-Ag nanocomposite modified GCE.

| Sample type | Added (μM) | Found (μM) | RSD (%) | Recovery (%) |
|---|---|---|---|---|
| Drinking water | 10 | 9.89 | 2.08 | 99.4 |
| Lake water | 10 | 10.02 | 1.66 | 101.9 |
| River water | 20 | 20.03 | 1.56 | 102.2 |
| Underground water | 20 | 20.01 | 0.39 | 100.1 |

## 4. CONCLUSION

In this work, a novel electrochemical 4-NP sensor was fabricated by a one-pot hydrothermal approach using GO and $AgNO_3$ as starting material. The proposed sensor displayed excellent electrocatalytic activity towards the detection of 4-NP with a linear detection range from 1 to 500 μM with a low detection limit of 0.114 μM. The fabricated sensor also showed an excellent anti-interference property and stability.

**Reference**


1. S. LacorteandD. Barcelo, *Environ. Sci. Technol.*, 28 (1994) 1159
2. A. Wang, H.P. Ng, Y. Xu, Y. Li, Y. Zheng, J. Yu, F. Han, F. PengandL. Fu, *Journal of Nanomaterials*, 2014 (2014) 6
3. L. Fu, Y. Zheng, Z. Wang, A. Wang, B. DengandF. Peng, *Digest Journal of Nanomaterials and Biostructures*, 10 (2015) 117
4. A. NiaziandA. Yazdanipour, *J. Hazard. Mater.*, 146 (2007) 421
5. C. Nistor, A. Oubiña, M.-P. Marco, D. BarcelóandJ. Emnéus, *Analytica chimica acta*, 426 (2001) 185
6. M.J. Thompson, L.N. Ballinger, S.E. CrossandM.S. Roberts, *Journal of Chromatography B: Biomedical Sciences and Applications*, 677 (1996) 117
7. A.L. Oliveira, E. Destandau, L. FougèreandM. Lafosse, *Food Chemistry*, 145 (2014) 522
8. E. Dorta, M. González, M.G. Lobo, C. Sánchez-MorenoandB. de Ancos, *Food Research International*, 57 (2014) 51
9. I. Navarro-González, R. González-Barrio, V. García-Valverde, A. Bautista-OrtínandM. Periago, *International Journal of Molecular Sciences*, 16 (2014) 805
10. R.T. Huang, Y.F. Lu, B.S. InbarajandB.H. Chen, *Journal of Functional Foods*, 12 (2015) 498
11. X. Guo, Z. WangandS. Zhou, *Talanta*, 64 (2004) 135
12. Y. Tang, R. Huang, C. Liu, S. Yang, Z. LuandS. Luo, *Analytical Methods*, 5 (2013) 5508
13. F. Xia, X. Xu, X. Li, L. Zhang, L. Zhang, H. Qiu, W. Wang, Y. LiuandJ. Gao, *Ind. Eng. Chem. Res.*, 53 (2014) 10576
14. L. Fu, Y. Zheng, Q. Ren, A. WangandB. Deng, *Journal of Ovonic Research*, 11 (2015) 21
15. L. Fu, Y.-H. ZhengandZ.-X. Fu, Ascorbic acid amperometric sensor using a graphene-wrapped hierarchical TiO2 nanocomposite, *Chemical Papers*, 2015, pp. 655.
16. A. Elzatahry, *Int. J. Electrochem. Sci*, 9 (2014) 22
17. E. Bettini, U. Kivisäkk, C. LeygrafandJ. Pan, *Int. J. Electrochem. Sci.*, 9 (2014) 61
18. J.B. Raoof, R. OjaniandS.R. Hosseini, *S. Afr. J. Chem.*, 66 (2013) 47
19. K.L. Wang, H. Wang, R.F. Wang, J.L. Key, V. LinkovandS. Ji, *S. Afr. J. Chem.*, 66 (2013) 86
20. Y. Zheng, A. Wang, H. Lin, L. FuandW. Cai, *RSC Advances*, 5 (2015) 15425
21. Y. Zheng, L. Fu, A. WangandW. Cai, *Int. J. Electrochem. Sci*, 10 (2015) 3530
22. H. Yin, Y. Zhou, S. Ai, X. Liu, L. ZhuandL. Lu, *Microchim Acta*, 169 (2010) 87
23. K. Singh, A.A. Ibrahim, A. Umar, A. Kumar, G.R. Chaudhary, S. SinghandS.K. Mehta, *Sensors and Actuators B: Chemical*, 202 (2014) 1044
24. K.S. Novoselov, A.K. Geim, S.V. Morozov, D. Jiang, Y. Zhang, S.V. Dubonos, I.V. GrigorievaandA.A. Firsov, *Science*, 306 (2004) 666
25. S. Stankovich, D.A. Dikin, G.H.B. Dommett, K.M. Kohlhaas, E.J. Zimney, E.A. Stach, R.D. Piner, S.T. NguyenandR.S. Ruoff, *Nature*, 442 (2006) 282
26. L. Fu, W. Cai, A.W. Wang, Y.H. Zheng, L. HeandZ.X. Fu, *Mater. Technol.*, 30 (2015) 264
27. L. Fu, A. Wang, Y. Zheng, W. CaiandZ. Fu, *Materials Letters*, 142 (2015) 119
28. L. FuandZ. Fu, *Ceram Int*, 41 (2015) 2492
29. L. Fu, W. Cai, A. WangandY. Zheng, *Materials Letters*, 142 (2015) 201
30. J. Li, D. Kuang, Y. Feng, F. Zhang, Z. XuandM. Liu, *J. Hazard. Mater.*, 201–202 (2012) 250
31. L. Mai, X. Xu, C. Han, Y. Luo, L. Xu, Y.A. WuandY. Zhao, *Nano Letters*, 11 (2011) 4992
32. L. ChuandX. Zhang, *Journal of Electroanalytical Chemistry*, 665 (2012) 26
33. W. Lu, R. Ning, X. Qin, Y. Zhang, G. Chang, S. Liu, Y. LuoandX. Sun, *J. Hazard. Mater.*, 197 (2011) 320
34. L. Fu, T. Xia, Y. Zheng, J. Yang, A. WangandZ. Wang, *Ceram Int*, 41 (2015) 5903
35. Y. Wu, W. Xu, Y. Wang, Y. YuanandR. Yuan, *Electrochimica Acta*, 88 (2013) 135
36. B. Zhao, Z. Liu, W. FuandH. Yang, *Electrochem. Commun.*, 27 (2013) 1

37. S. Park, J. An, R.D. Piner, I. Jung, D. Yang, A. Velamakanni, S.T. NguyenandR.S. Ruoff, *Chem. Mater.*, 20 (2008) 6592
38. W.S. HummersandR.E. Offeman, *J. Am. Chem. Soc.*, 80 (1958) 1339
39. L. Fu, Y. Zheng, A. Wang, W. CaiandH. Lin, *Food chemistry*, 181 (2015) 127
40. L. Fu, Y. Zheng, A. Wang, W. Cai, Z. FuandF. Peng, *Sensor Letters*, 13 (2015) 81
41. J.I. Paredes, S. Villar-Rodil, A. Martínez-AlonsoandJ.M.D. Tascón, *Langmuir*, 24 (2008) 10560
42. Y. Zhou, Q. Bao, L.A.L. Tang, Y. ZhongandK.P. Loh, *Chem. Mater.*, 21 (2009) 2950
43. L. Fu, Y. ZhengandA. Wang, *Int. J. Electrochem. Sci*, 10 (2015) 3518
44. J. Xu, K. Wang, S.-Z. Zu, B.-H. HanandZ. Wei, *ACS Nano*, 4 (2010) 5019
45. B. Li, T. Liu, Y. WangandZ. Wang, *Journal of colloid and interface science*, 377 (2012) 114
46. T. Nakajima, A. MabuchiandR. Hagiwara, *Carbon*, 26 (1988) 357
47. D. Chen, L. LiandL. Guo, *Nanotechnology*, 22 (2011)
48. M.R. Guascito, D. Chirizzi, R.A. Picca, E. MazzottaandC. Malitesta, *Materials Science and Engineering: C*, 31 (2011) 606
49. J. Li, D. Kuang, Y. Feng, F. Zhang, Z. Xu, M. LiuandD. Wang, *Biosens. Bioelectron.*, 42 (2013) 198